Table 5. Frequencies of the Complement Factor B (*CFB*) rs641153 Genotype in AMD and Control Groups and Genotype Effects of Studies Included in the Meta-Analysis, 2006–2011

First Author, Year (Reference No.)	No. of Subjects								Genotype Effect			
	AMD				Non-AMD Group				AA vs. GG		GA vs. GG	
	AA	GA	GG	Total	AA	GA	GG	Total	OR_1[a]	95% CI	OR_2	95% CI
Caucasians												
Maller, 2008 (13)	3	106	1,129	1,238	10	171	753	934	0.20	0.06, 0.73	0.41	0.32, 0.53
Gold, 2006 (32)	2	52	497	551	3	53	213	269	0.29	0.05, 1.72	0.42	0.28, 0.64
Spencer, 2007 (36)	2	66	630	698	3	50	229	282	0.24	0.04, 1.46	0.48	0.32, 0.71
Scholl, 2008 (26)	0	6	106	112	0	10	57	67	0.54	0.01, 27.57	0.32	0.11, 0.93
Farwick, 2009 (31)	0	26	750	776	0	26	93	119	0.12	0.002, 6.32	0.12	0.07, 0.22
Reynolds, 2009 (24)	0	6	97	103	0	11	46	57	0.48	0.01, 24.41	0.26	0.09, 0.74
Richardson, 2009 (35)	2	54	473	529	3	41	155	199	0.22	0.04, 1.32	0.43	0.28, 0.67
Seddon, 2009 (27)	0	23	256	279	6	138	1,023	1,167	0.31	0.02, 5.47	0.67	0.42, 1.06
McKay, 2009 (34)	3	33	389	425	5	86	337	428	0.52	0.12, 2.19	0.33	0.22, 0.51
Chen, 2011 (54)	3	128	1,204	1,335	4	83	422	509	0.26	0.06, 1.18	0.54	0.40, 0.73
Pooled data	15	500	5,531	6,046	34	669	3,328	4,031	0.26	0.14, 0.48	0.42	0.37, 0.48
Asians												
Chu, 2008 (56)	1	30	113	144	4	32	90	126	0.20	0.02, 1.81	0.75	0.42, 1.32
Pei, 2009 (23)	0	18	105	123	0	18	112	130	1.07	0.02, 54.23	1.07	0.53, 2.16
Kaur, 2010 (37)	2	18	142	162	10	53	95	158	0.13	0.03, 0.62	0.23	0.13, 0.41
Liu, 2010 (55)	0	17	221	238	1	25	194	220	0.29	0.01, 7.23	0.60	0.31, 1.14
Pooled data	3	83	581	667	15	128	491	634	0.17	0.05, 0.59	0.55	0.41, 0.74

Abbreviations: AMD, age-related macular degeneration; CI, confidence interval; OR, odds ratio.
[a] Continuing correction was performed by adding 0.5 in all cells for OR_1.

the "flip-flop" phenomenon, in which varying LD structure between different populations leads to a flip in the direction of the allelic effect, presumably because the genotyped SNP is tagging the causative allele, and different marker alleles are in LD with the causative allele across different populations (58–60). However, the C allele in the Indian population was consistent in having a protective association, similar to other ethnic groups, which did not fit with the "flip-flop" phenomenon.

These genetic associations are very similar to the ones recently described in a meta-analysis of genome-wide association studies for AMD (61); the allele effect for *C2* rs9332739 was 0.46, and the allele effect for *CFB* rs641153 was 0.54. These pooled estimates were derived from over 2,500 cases and over 4,100 controls, and the consistency of the results shows that this effect size is robust.

Multilocus associations

Although some studies had assessed compound genotype effects of the 2 SNPs in *C2* and *CFB*, the way in which investigators had reported their data did not allow us to pool haplotype effects. Previous reports show nearly complete LD between *C2* rs9332739 and *CFB* rs4151667 (r = 0.91–1.00) (32–34) and separately between *C2* rs547154 and *CFB* rs641153 (r = 0.92–0.96) (35, 36), indicative of dependent genetic effects. Given that all 4 SNPs showed similar magnitudes of genetic effects, identification of functional causal variants from the existing data would be difficult and might require very diverse populations with smaller LD blocks to isolate functional regions. This is a timely reminder that distance is a poor proxy for LD; the 2 SNPs examined here in *CFB* are only 156 base pairs apart and are not in LD (r^2 = 0.004), yet rs641153 in *CFB* is in complete LD with rs547154 in *C2*, which is 3,242 base pairs away (http://hapmap.ncbi.nlm.nih.gov/). Likewise, the 2 SNPs in *C2*, which are 7,134 base pairs apart, are not in LD (r^2 = 0.004), but rs9332739 in *C2* is in complete LD with rs 4151667 in *CFB*, which is 10,220 base pairs away.

The fact that 2 LD blocks are equally powerful markers for AMD risk but are independent of each other leads to the possibility that they are both tagging a causative SNP that is not in either LD block. Fine mapping or next-generation sequencing may shed more light on this possibility.

Burden of disease

The *C2* and *CFB* polymorphisms analyzed here contribute only 2%–6% of the population risk of AMD. In terms of public health prevention, focusing on smoking cessation would carry a much greater benefit, with a PAR of 36.9% (34), and stronger genetic loci, such as *CFH*, carry a much greater PAR (i.e., 58.9%) (11). Some groups of researchers have combined the PAR of the 14 variants identified to obtain much larger and clinically useful estimates (61) in

an attempt to develop a genetic risk score (27). Others have generated haplotypes, which is concordant with the evolving view that this could represent a more robust method of analysis (35).

Strengths and weaknesses

This study had a number of strengths. We followed a rigorous protocol of systematic review, identifying data from 3 different databases. Data extraction was carried out in duplicate. We pooled allele frequencies and genetic effects separately, as suggested by the guidelines of the Human Genome Epidemiology Network (62). We pooled effects using a model-free method, which allows the data to suggest which genetic mode of action might be at work. We thoroughly investigated heterogeneity and study-size effects and estimated the PAR. However, we could not assess haplotype effects, which would have required individual patient data or compound genotype summary data. Another potential drawback is that the majority of the studies were clinic-based case-control studies, which might have produced overestimation of the genetic association. This bias could be avoided through the use of population-based nested case-control studies, but these types of studies are few, because it is costly to perform examinations and fundus photographs on thousands of people to determine who has early signs of AMD. In addition, few people would have advanced AMD in such studies.

In summary, our meta-analysis provides evidence for an association between *C2/CFB* polymorphisms and AMD. Carriage of preventive alleles for *C2* rs9332739 and rs547154 would decrease the risk of AMD in Caucasians by approximately 45% and 53%, respectively; carriage of preventive alleles for *CFB* rs415667 and rs641153 would decrease it by approximately 46% and 59%. These allele effects contribute to an absolute lowering of the risk of all AMD in general Caucasian populations by 2.0%–6.0%. Although these associations appear consistent in Caucasian and Asian ethnic groups, the data are still sparse, and further studies are required to estimate the effects in non-Caucasian ethnic groups with more precision. Early work indicates that these polymorphisms may affect binding affinities (e.g., between *CFB* and *C3b* (63, 64)), promoting or retarding the complement cascade; however, better understanding of the full functional implications of these alleles will require more research.

ACKNOWLEDGMENTS

Author affiliations: Section for Clinical Epidemiology and Biostatistics, Faculty of Medicine, Ramathibodi Hospital, Mahidol University, Bangkok, Thailand (Ammarin Thakkinstian); Centre for Clinical Epidemiology and Biostatistics, University of Newcastle, Newcastle, New South Wales, Australia (Mark McEvoy, John Attia); Centre for Public Health, Queen's University of Belfast, Belfast, United Kingdom (Usha Chakravarthy, Gareth J. McKay, Giuliana Silvestri); Brien Holden Eye Research Centre, L. V. Prasad Eye Institute, Hyderabad, India (Subhabrata Chakrabarti, Inderjeet Kaur); Department of Health Sciences Research, Mayo Clinic, Rochester, Minnesota (Euijung Ryu); Macular Degeneration Center, Casey Eye Institute, Oregon Health and Science University, Portland, Oregon (Peter Francis); Division of Molecular and Cellular Biology, National Institute of Sensory Organs, National Hospital Organization Tokyo Medical Center, Tokyo, Japan (Takeshi Iwata, Masakazu Akahori); Leibniz Institute of Arteriosclerosis Research, Münster, Germany (Astrid Arning); Institute of Molecular Biology, University of Oregon, Eugene, Oregon (Albert O. Edwards); Ophthalmic Epidemiology and Genetics Service, Department of Ophthalmology, Tufts University School of Medicine and Tufts Medical Center, Boston, Massachusetts (Johanna M. Seddon); and John Hunter Hospital and Hunter Medical Research Institute, Newcastle, New South Wales, Australia (John Attia).

Conflict of interest: none declared.

REFERENCES

1. Klein ML, Schultz DW, Edwards A, et al. Age-related macular degeneration: clinical features in a large family and linkage to chromosome 1q. *Arch Ophthalmol.* 1998;116(8):1082–1088.
2. Mitchell P, Smith W, Attebo K, et al. Prevalence of age-related maculopathy in Australia. The Blue Mountains Eye Study. *Ophthalmology.* 1995;102(10):1450–1460.
3. Pang CP, Baum L, Chan WM, et al. The apolipoprotein E ε4 allele is unlikely to be a major risk factor of age-related macular degeneration in Chinese. *Ophthalmologica.* 2000;214(4):289–291.
4. VanNewkirk MR, Nanjan MB, Wang JJ, et al. The prevalence of age-related maculopathy: the Visual Impairment Project. *Ophthalmology.* 2000;107(8):1593–1600.
5. Evans J, Wormald R. Is the incidence of registrable age-related macular degeneration increasing? *Br J Ophthalmol.* 1996;80(1):9–14.
6. Schmidt S, Klaver C, Saunders A, et al. A pooled case-control study of the apolipoprotein E (*APOE*) gene in age-related maculopathy. *Ophthalmic Genet.* 2002;23(4):209–223.
7. Vingerling JR, Dielemans I, Hofman A, et al. The prevalence of age-related maculopathy in the Rotterdam Study. *Ophthalmology.* 1995;102(2):205–210.
8. Rivera A, Fisher SA, Fritsche LG, et al. Hypothetical *LOC387715* is a second major susceptibility gene for age-related macular degeneration, contributing independently of complement factor H to disease risk. *Hum Mol Genet.* 2005;14(21):3227–3236.
9. Conley YP, Jakobsdottir J, Mah T, et al. *CFH, ELOVL4, PLEKHA1* and *LOC387715* genes and susceptibility to age-related maculopathy: AREDS and CHS cohorts and meta-analyses. *Hum Mol Genet.* 2006;15(21):3206–3218.
10. Despriet DD, Klaver CC, Witteman JC, et al. Complement factor H polymorphism, complement activators, and risk of age-related macular degeneration. *JAMA.* 2006;296(3):301–309.
11. Thakkinstian A, Han P, McEvoy M, et al. Systematic review and meta-analysis of the association between complement factor H *Y402H* polymorphisms and age-related macular degeneration. *Hum Mol Genet.* 2006;15(18):2784–2790.

12. Kaur I, Katta S, Hussain A, et al. Variants in the 10q26 gene cluster (*LOC387715* and *HTRA1*) exhibit enhanced risk of age-related macular degeneration along with *CFH* in Indian patients. *Invest Ophthalmol Vis Sci.* 2008;49(5):1771–1776.
13. Maller J, George S, Purcell S, et al. Common variation in three genes, including a noncoding variant in *CFH*, strongly influences risk of age-related macular degeneration. *Nat Genet.* 2006;38(9):1055–1059.
14. Maller JB, Fagerness JA, Reynolds RC, et al. Variation in complement factor 3 is associated with risk of age-related macular degeneration. *Nat Genet.* 2007;39(10):1200–1201.
15. Bergeron-Sawitzke J, Gold B, Olsh A, et al. Multilocus analysis of age-related macular degeneration. *Eur J Hum Genet.* 2009;17(9):1190–1199.
16. Cui L, Zhou H, Yu J, et al. Noncoding variant in the complement factor H gene and risk of exudative age-related macular degeneration in a Chinese population. *Invest Ophthalmol Vis Sci.* 2010;51(2):1116–1120.
17. Despriet DD, van Duijn CM, Oostra BA, et al. Complement component C3 and risk of age-related macular degeneration. *Ophthalmology.* 2009;116(3):474.e2–480.e2.
18. Edwards AO, Fridley BL, James KM, et al. Evaluation of clustering and genotype distribution for replication in genome wide association studies: the Age-Related Eye Disease Study. *PLoS One.* 2008;3(11):e3813. (doi:10.1371/journal.pone.0003813).
19. Francis PJ, Hamon SC, Ott J, et al. Polymorphisms in *C2*, *CFB* and *C3* are associated with progression to advanced age related macular degeneration associated with visual loss. *J Med Genet.* 2009;46(5):300–307.
20. Goto A, Akahori M, Okamoto H, et al. Genetic analysis of typical wet-type age-related macular degeneration and polypoidal choroidal vasculopathy in Japanese population. *J Ocul Biol Dis Infor.* 2009;2(4):164–175.
21. Gu J, Pauer GJ, Yue X, et al. Assessing susceptibility to age-related macular degeneration with proteomic and genomic biomarkers. *Mol Cell Proteomics.* 2009;8(6):1338–1349.
22. Park KH, Fridley BL, Ryu E, et al. Complement component 3 (*C3*) haplotypes and risk of advanced age-related macular degeneration. *Invest Ophthalmol Vis Sci.* 2009;50(7):3386–3393.
23. Pei XT, Li XX, Bao YZ, et al. Association of c3 gene polymorphisms with neovascular age-related macular degeneration in a Chinese population. *Curr Eye Res.* 2009;34(8):615–622.
24. Reynolds R, Hartnett ME, Atkinson JP, et al. Plasma complement components and activation fragments: associations with age-related macular degeneration genotypes and phenotypes. *Invest Ophthalmol Vis Sci.* 2009;50(12):5818–5827.
25. Scholl HP, Fleckenstein M, Fritsche LG, et al. *CFH*, *C3* and *ARMS2* are significant risk loci for susceptibility but not for disease progression of geographic atrophy due to AMD. *PLoS One.* 2009;4(10):e7418. (doi:10.1371/journal.pone.0007418).
26. Scholl HP, Charbel Issa P, Walier M, et al. Systemic complement activation in age-related macular degeneration. *PLoS One.* 2008;3(7):e2593. (doi:10.1371/journal.pone.0002593).
27. Seddon JM, Reynolds R, Maller J, et al. Prediction model for prevalence and incidence of advanced age-related macular degeneration based on genetic, demographic, and environmental variables. *Invest Ophthalmol Vis Sci.* 2009;50(5):2044–2053.
28. Seitsonen SP, Onkamo P, Peng G, et al. Multifactor effects and evidence of potential interaction between complement factor H *Y402H* and *LOC387715* A69S in age-related macular degeneration. *PLoS One.* 2008;3(12):e3833. (doi:10.1371/journal.pone.0003833).
29. Spencer KL, Olson LM, Anderson BM, et al. *C3* R102G polymorphism increases risk of age-related macular degeneration. *Hum Mol Genet.* 2008;17(12):1821–1824.
30. Yates JR, Sepp T, Matharu BK, et al. Complement *C3* variant and the risk of age-related macular degeneration. *N Engl J Med.* 2007;357(6):553–561.
31. Farwick A, Dasch B, Weber BH, et al. Variations in five genes and the severity of age-related macular degeneration: results from the Muenster Aging and Retina Study. *Eye (Lond).* 2009;23(12):2238–2244.
32. Gold B, Merriam JE, Zernant J, et al. Variation in factor B (*BF*) and complement component 2 (*C2*) genes is associated with age-related macular degeneration. *Nat Genet.* 2006;38(4):458–462.
33. Jakobsdottir J, Conley YP, Weeks DE, et al. *C2* and *CFB* genes in age-related maculopathy and joint action with *CFH* and *LOC387715* genes. *PLoS One.* 2008;3(5):e2199. (doi:10.1371/journal.pone.0002199).
34. McKay GJ, Silvestri G, Patterson CC, et al. Further assessment of the complement component 2 and factor B region associated with age-related macular degeneration. *Invest Ophthalmol Vis Sci.* 2009;50(2):533–539.
35. Richardson AJ, Amirul Islam FM, Guymer RH, et al. Analysis of rare variants in the complement component 2 (*C2*) and factor B (*BF*) genes refine association for age-related macular degeneration (AMD). *Invest Ophthalmol Vis Sci.* 2009;50(2):540–543.
36. Spencer KL, Hauser MA, Olson LM, et al. Protective effect of complement factor B and complement component 2 variants in age-related macular degeneration. *Hum Mol Genet.* 2007;16(16):1986–1992.
37. Kaur I, Katta S, Reddy RK, et al. The involvement of complement factor B and complement component C2 in an Indian cohort with age-related macular degeneration. *Invest Ophthalmol Vis Sci.* 2010;51(1):59–63.
38. Thakkinstian A, McKay GJ, McEvoy M, et al. Systematic review and meta-analysis of the association between complement component 3 and age-related macular degeneration: a HuGE review and meta-analysis. *Am J Epidemiol.* 2011;173(12):1365–1379.
39. Thakkinstian A, Thompson JR, Minelli C, et al. Choosing between per-genotype, per-allele, and trend approaches for initial detection of gene-disease association. *J Appl Stats.* 2009;36(6):633–646.
40. Thakkinstian A, McEvoy M, Minelli C, et al. Systematic review and meta-analysis of the association between β_2-adrenoceptor polymorphisms and asthma: a HuGE review. *Am J Epidemiol.* 2005;162(3):201–211.
41. Thompson JR, Minelli C, Abrams KR, et al. Meta-analysis of genetic studies using Mendelian randomization—a multivariate approach. *Stat Med.* 2005;24(14):2241–2254.
42. Thompson SG. Why sources of heterogeneity in meta-analysis should be investigated. *BMJ.* 1994;309(6965):1351–1355.
43. Thompson SG, Sharp SJ. Explaining heterogeneity in meta-analysis: a comparison of methods. *Stat Med.* 1999;18(20):2693–2708.
44. Thompson SG, Smith TC, Sharp SJ. Investigating underlying risk as a source of heterogeneity in meta-analysis. *Stat Med.* 1997;16(23):2741–2758.

45. Minelli C, Thompson JR, Abrams KR, et al. The choice of a genetic model in the meta-analysis of molecular association studies. *Int J Epidemiol.* 2005;34(6):1319–1328.
46. Egger M, Davey Smith G, Schneider M, et al. Bias in meta-analysis detected by a simple, graphical test. *BMJ.* 1997;315(7109):629–634.
47. Palmer TM, Peter JL, Sutton AJ, et al. Contour-enhanced funnel plots in meta-analysis. *STATA J.* 2008;8(2):242–254.
48. Peters JL, Sutton AJ, Jones DR, et al. Contour-enhanced meta-analysis funnel plots help distinguish publication bias from other causes of asymmetry. *J Clin Epidemiol.* 2008; 61(10):991–996.
49. Duval S, Tweedie R. Trim and fill: a simple funnel-plot-based method of testing and adjusting for publication bias in meta-analysis. *Biometrics.* 2000;56(2):455–463.
50. Hayden KM, Zandi PP, Lyketsos CG, et al. Apolipoprotein E genotype and mortality: findings from the Cache County Study. *J Am Geriatr Soc.* 2005;53(6):935–942.
51. Rossman MD, Thompson B, Frederick M, et al. HLA-DRB1*1101: a significant risk factor for sarcoidosis in blacks and whites. *Am J Hum Genet.* 2003;73(4):720–735.
52. StataCorp LP. *Stata Statistical Software: Release 11.0.* College Station, TX: StataCorp LP; 2009.
53. Spiegelhalter D, Thomas A, Best N, et al. *WinBUGS User Manual.* Cambridge, United Kingdom: MRC Biostatistics Unit, Institute of Public Health, University of Cambridge; 2007.
54. Chen Y, Zeng J, Zhao C, et al. Assessing susceptibility to age-related macular degeneration with genetic markers and environmental factors. *Arch Ophthalmol.* 2011;129(3): 344–351.
55. Liu X, Zhao P, Tang S, et al. Association study of complement factor H, *C2*, *CFB*, and *C3* and age-related macular degeneration in a Han Chinese population. *Retina.* 2010;30(8):1177–1184.
56. Chu J, Zhou CC, Lu N, et al. Genetic variants in three genes and smoking show strong associations with susceptibility to exudative age-related macular degeneration in a Chinese population. *Chin Med J (Engl).* 2008;121(24): 2525–2533.
57. Ioannidis JP, Ntzani EE, Trikalinos TA. 'Racial' differences in genetic effects for complex diseases. *Nat Genet.* 2004;36(12):1312–1318.
58. Clarke GM, Cardon LR. Aspects of observing and claiming allele flips in association studies. *Genet Epidemiol.* 2010;34 (3):266–274.
59. Zaykin DV, Shibata K. Genetic flip-flop without an accompanying change in linkage disequilibrium [letter]. *Am J Hum Genet.* 2008;82(3):794–796.
60. Lin PI, Vance JM, Pericak-Vance MA, et al. No gene is an island: the flip-flop phenomenon. *Am J Hum Genet.* 2007;80(3):531–538.
61. Yu Y, Bhangale TR, Fagerness J, et al. Common variants near *FRK/COL10A1* and *VEGFA* are associated with advanced age-related macular degeneration. *Hum Mol Genet.* 2011;20(18):3699–3709.
62. Little J, Higgins J, eds. *The HuGENet™ HuGE Review Handbook, Version 1.0.* Ottawa, Ontario, Canada: University of Ottawa; 2006.
63. Heurich M, Martínez-Barricarte R, Francis NJ, et al. Common polymorphisms in *C3*, factor B, and factor H collaborate to determine systemic complement activity and disease risk. *Proc Natl Acad Sci U S A.* 2011;108(21):8761–8766.
64. Montes T, Tortajada A, Morgan BP, et al. Functional basis of protection against age-related macular degeneration conferred by a common polymorphism in complement factor B. *Proc Natl Acad Sci U S A.* 2009;106(11):4366–4371.
65. Seddon JM, Sharma S, Adelman RA. Evaluation of the Clinical Age-Related Maculopathy Staging System. *Ophthalmology.* 2006;113(2):260–266.

APPENDIX

Search strategy used for EMBASE (Ovid)

1. Gene
2. Allele
3. Polymorphism
4. Macular degeneration
5. Complement component 2
6. Complement factor 2
7. Component 2
8. C2
9. Complement factor B
10. Component B
11. CFB
12. FB
13. (1 *OR* 2 *OR* 3)
14. (5 *OR* 6 *OR* 7 *OR* 8)
15. (9 *OR* 10 *OR* 11 *OR* 12)
16. 13 *AND* 4 *AND* (14 *OR* 15)

Search strategy used for Scopus

[(ALL("gene") *OR* ALL("allele") *OR* ALL("polymorphism")] *AND* [ALL("macular degeneration")] *AND* [(ALL ("complement component 2") *OR* ALL("complement factor 2") *OR* ALL("c2") *OR* ALL("component 2")] *OR* [ALL("complement factor B") *OR* ALL("component B") *OR* ALL("cfb") *OR* ALL("bf")] *AND* [LIMIT-TO(SUBJAREA, "MEDI") *OR* LIMIT-TO(SUBJAREA, "BIOC")] *AND* [EXCLUDE(SUBJAREA, "NEUR") *OR* EXCLUDE (SUBJAREA, "IMMU") *OR* EXCLUDE(SUBJAREA, "AGRI")] *AND* [EXCLUDE(SUBJAREA, "MULT") *OR* EXCLUDE(SUBJAREA, "PHAR") *OR* EXCLUDE(SUBJAREA, "CHEM")].

三宅病研究の現状と展望

Miyake's disease

角田和繁

Abstract

Miyake's disease (occult macular dystrophy: OMD) was first described by Miyake et al. to be a hereditary macular dystrophy without visible fundus abnormalities. Patients with OMD are characterized by a progressive decrease of visual acuity with normal appearing fundus and normal fluorescein angiograms. The important signs of OMD are normal full-field electroretinograms (ERGs) but abnormal focal macular ERGs. In 2010, we found that dominant mutations in the *RP1L1* gene were responsible for OMD by a linkage analysis of two OMD families, and recently, the same mutations were known to cause OMD in non-Japanese patients. Here, we describe how this disorder has been discovered and the causative gene was found by Miyake's group, together with the detailed characteristics of OMD.

Key words: Miyake's disease, occult macular dystrophy, *RP1L1*

はじめに

眼科疾患において，日本人がその発見および疾患概念の確立に大きく貢献した例が幾つか知られている．小口病は1907年に眼科医 小口忠太によって発見された先天性の停止性夜盲症であり[1]，現在でも 'Oguchi's disease' という呼称が世界的に用いられている．また，網膜血管異常を発端として大動脈炎の病態が明らかになった 'Takayasu's arteritis'，およびメラノサイトに対する自己免疫疾患である 'Vogt-Koyanagi-Harada disease' などについても，それぞれ発見に関与した日本人眼科医である，高安右人，小柳美三，原田永之助の名前が用いられている．

1990年に網膜色素変性の原因遺伝子としてロドプシンが同定されて以来[2]，多くの遺伝性網膜疾患についてその原因遺伝子が明らかとなり，現在では若年性の網膜色素変性（レーベル先天黒内障）に対して遺伝子治療が行われるまでとなった．前述の小口病に関しても，1995年に原因遺伝子としてアレスチンが同定されたが[3]，これは日本人患者から得られたDNAをもとに，ドイツの研究者の手によって成し得た研究成果であった．

三宅病，すなわちオカルト黄斑ジストロフィーとは，1989年に名古屋大学の三宅養三によって '眼底所見に異常のみられない家族性黄斑症' として初めて紹介された疾患である[4,5]．その後，その疾患原因については長い間不明のままであったが，発見からほぼ20年を経過した2010年になって，本疾患の原因遺伝子として8番染色体短腕に *RP1L1* (*RP1-LIKE PROTEIN 1*) が特定された[6]．この疾患は黄斑部局所網膜電図（ERG）の開発からそれによる疾患概念の確立，

Kazushige Tsunoda: Laboratory of Visual Physiology, National Institute of Sensory Organs 国立病院機構東京医療センター臨床研究センター 視覚生理研究室

0047-1852/13/¥60/頁/JCOPY

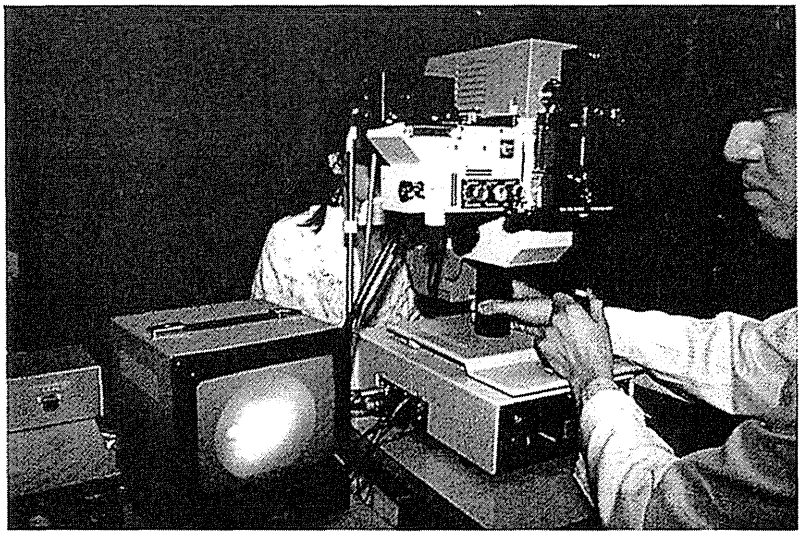

図1　名古屋大学で製作された黄斑部局所ERGの1号機
手前のモニターに赤外光による眼底像と刺激部位が映し出されている
(写真提供は三宅養三教授のご厚意による).

そして原因遺伝子の解明までをすべて日本国内の研究グループによって完結させた初めての眼科疾患であり，現在では'三宅病(Miyake's disease)'という呼称が用いられるようになってきている[7,8].

本稿では，三宅病がどのようにして発見されたのか，また，その疾患の特徴および現在までの研究状況についてまとめてみた.

1. 三宅病が発見されるまで
—黄斑部局所ERGの開発—

三宅はボストンに留学中，Hiroseらとともに黄斑部局所からERGを記録する研究に従事していた．それまでにも同様の試みは世界で行われていたが，臨床でルーチンに利用されるには至っていなかった[9,10]．当時ボストンでは，細隙灯顕微鏡にレーザー光刺激を備え付けた装置を試作していたが，眼底を観察するための背景光が強くノイズも多く，結局実用化されなかった．三宅は名古屋大学に帰室後，キャノン社の協力を得て，赤外線眼底カメラの光路に光刺激(ハロゲン)と背景光(タングステン)を組み込み，網膜の局所刺激でERGと視覚誘発電位(VEP)を同時記録する装置を試作した．眼底は赤外線でモニターされるため，ボストンの装置と異なり被験者は検査中もまぶしくなく，安定した反応が記録された(**図1**)．その後，更に改良を加えたうえで正常被験者や様々な黄斑部疾患の患者から膨大な数の黄斑部局所ERG記録が行われ，そのデータの信頼性が確かめられた[11-16]．黄斑部局所ERGの大きな特長は，網膜上の測定したい部位に刺激光を移動でき，刺激サイズも変えられること．また，a波，b波，OP波，off波など，全視野ERGと同質の波形成分が得られ，各波形の変化によって疾患の病態を把握することができるということである.

当時三宅は外勤先の病院で原因不明の視力低下をきたしている29歳女性を診察していた．その患者は過去に複数の大学病院を含む多くの施設で，心因性視力障害，視神経疾患，中枢性疾患等々の診断を受けていた．全視野ERGは既に正常であるとわかっていたが，患者と様々な話をするうえで，三宅は直感的に網膜疾患を疑ったという．その根拠は，彼女が黒板よりも特に白板に書かれた文字を読みにくいと訴えており，これは網膜疾患に多くみられる訴えであることと，彼女と接した雰囲気で心因性の可能性はないと感じられたことなどだという．三宅はその患者をすぐに名古屋大学に連れて行き，自身で黄斑部局所ERGを記録したところ，黄斑部の反応が選択的に低下していることを発見した．これには三宅自身も大変驚き，その家族

を調べたところ常染色体優性遺伝と思われる疾患家系であることがわかった．これらの症例が‘hereditary macular dystrophy without visible fundus abnormality(眼底所見に異常のみられない家族性黄斑ジストロフィー)’として1989年にAmerican Journal of Ophthalmologyに発表された[4]．その後，眼底所見が正常である(＝異常が隠れている)ことから，オカルト(＝目に見えない)黄斑ジストロフィーと命名された[5]．この疾患を契機に三宅らは，原因不明の視力低下を訴える症例にできるだけ黄斑部局所ERG記録を行ったところ，この範疇に入る疾患が少なくないことを知った．他の既知の黄斑ジストロフィー(例えばスターガルト病，Best病等々)と比べても，少なくとも我が国では本疾患の頻度は少なくないとの印象をもたれたとのことである．

その後，Sutterらにより開発された多局所ERGが市販化され，1990年代半ば以降には国内でも多くの大学病院で採用されるようになっていった[17]．それに伴い三宅病の報告も国内外で多数みられるようになった[18-28]．

2．三宅病の特徴的な症状と経過

黄斑部，特に中心窩の視細胞機能が局所的に低下するため，視力低下および中心比較暗点が主な症状である．問診の際に羞明を訴える患者も多いが，印象としては錐体ジストロフィーや杆体一色覚など錐体機能不全の患者が訴えるような強い羞明ではない．進行は非常にゆっくりであるため，自覚症状の出るかなり以前から黄斑部の機能低下は始まっていると考えられる．自覚症状を訴える時期は10歳頃～60歳前後までと非常に幅があり，両眼の視力が極めてゆっくりと低下していく．発症には男女による違いはなく，また屈折にも特に傾向はない．

両眼がほぼ同時に進行する例が多いが，自覚症状の出現や視力低下の進行が，左右眼で数年から10年近く異なるケースもある．ただし，自覚症状が片眼のみの患者でも，黄斑部におけるERGの振幅は既に両眼で低下している．

根本的な治療法はない．視力低下が進行すると当然識字困難となるが，ほとんどの患者は拡大鏡などを用いることにより十分に日常の読み書きをこなしている．個人的な見解ではあるが，この疾患の場合，同一視力を有する他の網膜疾患の患者に比べて見え方の‘質’が良いという印象を受ける．また周辺視力は末期でも正常に保たれるため，歩行時にもそれほどの困難は生じない．

常染色体優性遺伝の疾患であるため，典型的な症例では両親のどちらかに同様の症状をもつ者がいる．ただし，後述するように孤発例の報告も多い．

以下に，典型例(28歳，男性)の症状経過を示す．

[主訴]　両眼の霧視

[経過]　18歳時，左眼がぼやけていることに気づく．眼鏡店で眼科受診を勧められたが放置していた．

23歳時，大学病院を受診．矯正視力は右1.2，左0.8．左眼視力不良の原因はわからないといわれた．

26歳時，右眼にも同様の見えにくさを自覚した．時に羞明を自覚する．

28歳時，次第に見えにくさが進行するため再び大学病院を受診．ERG，VEPなどの検査を行うも異常を指摘されなかった．その後東京医療センターを受診し，電気生理学的検査にて三宅病と診断された．更に遺伝子検査により*RP1L1*変異(p.Arg45Trp)が確認された．

[家族歴]　母に若い頃から同様の症状あり．父および2人の姉には症状なし．

[検査所見]　矯正視力：(電光表示の視力表)右(0.7)，左(0.4)．(字ひとつ視力)　右(1.0)，左(0.6)．ハンフリー自動視野計：中心10度の測定にて，比較暗点を認める．

眼底写真，網膜自発蛍光，光干渉断層計(OCT)：(**図2**)．

全視野ERG，多局所ERG，黄斑部局所ERG：(**図3**)．

3．三宅病の診断に必要な検査

1）自覚的検査

矯正視力は，通常は運転免許の取得に問題の

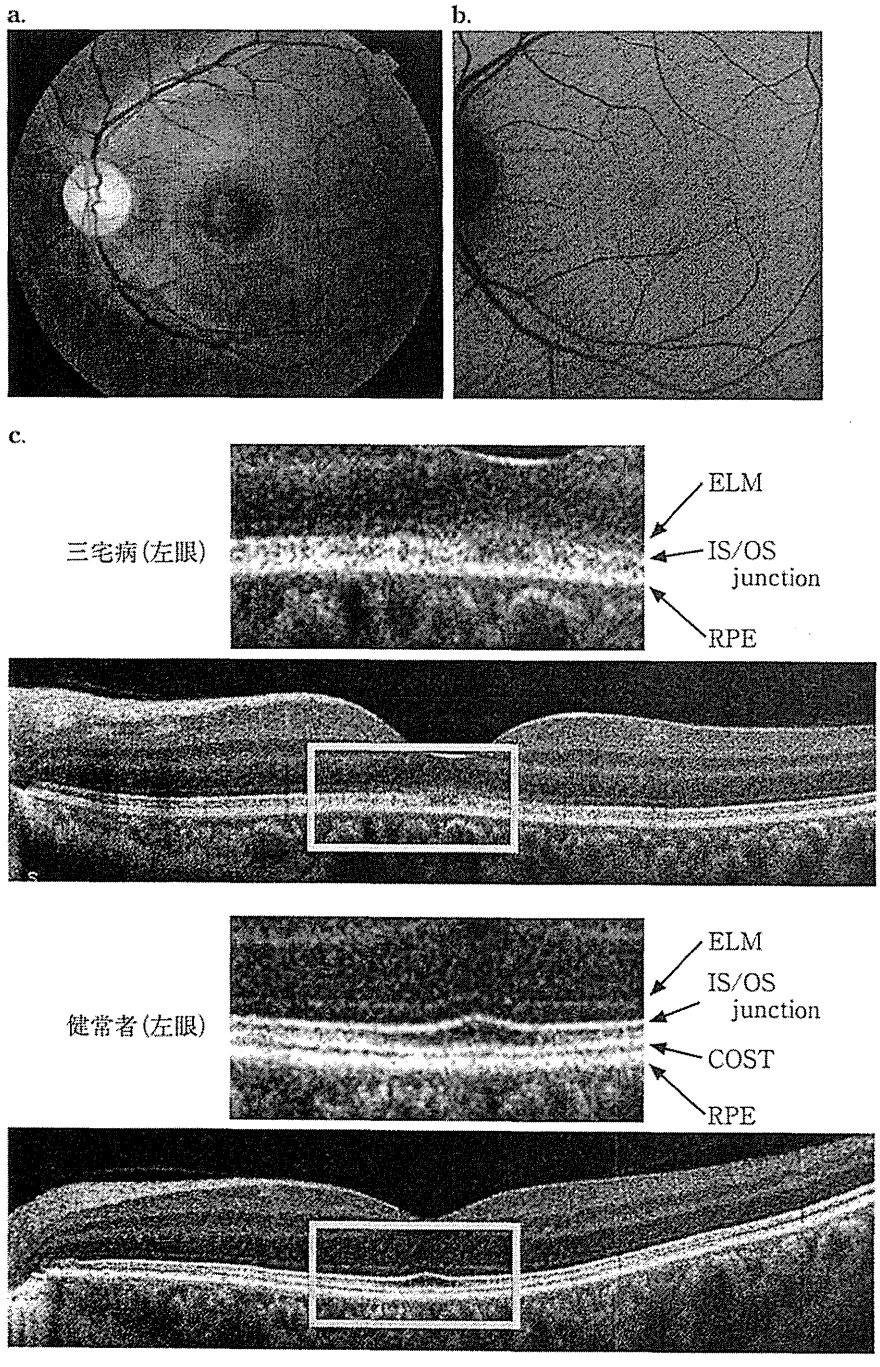

図2 典型例(28際, 男性)の画像所見

眼底写真(a), 網膜自発蛍光(b)はいずれも正常. 光干渉断層計(OCT)(c)では, 黄斑部における錐体視細胞外節先端部(cone outer segment tip: COST)ラインの消失, 視細胞内節外節接合部(photoreceptor inner segment/outer segment junction: IS/OS)ラインの不明瞭化がみられる.

生じる0.7未満に低下してから受診する場合が多いが, 初期には1.2と良好なケースもある. 視力障害は徐々に進行し, 最終的に0.1-0.2程度まで低下することがある. ただし他の黄斑ジストロフィーと異なり網膜色素上皮の萎縮をきたすことがないため, 最終視力が0.1を下回るケースはない(図4). 80歳の時点でも1.0の視力を維持している患者もおり, 進行には大きな個体差がある.

羞明を伴うケースでは, 電光掲示板を使った

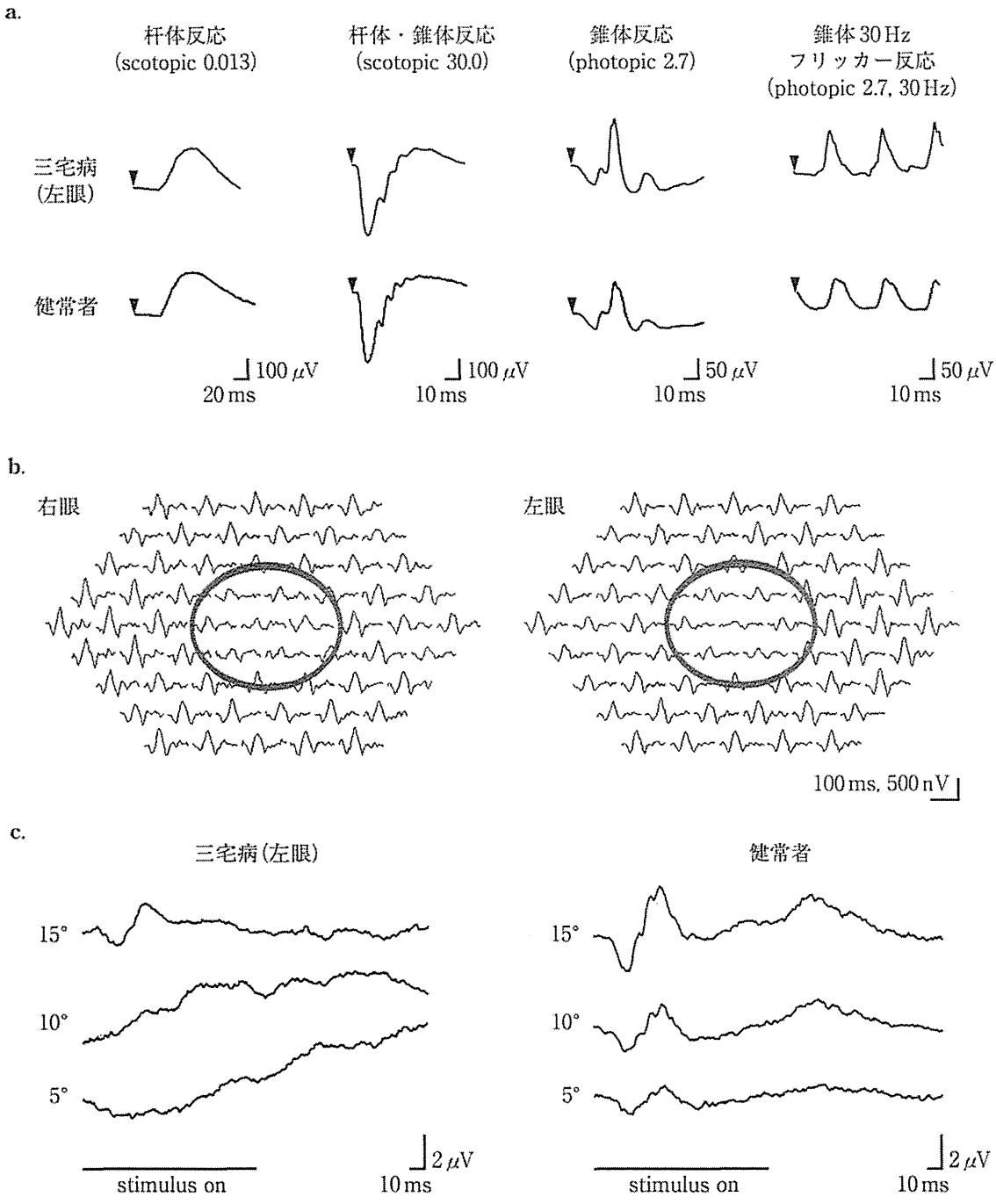

図3　図2と同一患者の電気生理学的検査所見

全視野ERG(a)では，杆体系，錐体系ともに正常反応を示している．多局所ERG(b)では黄斑部における振幅低下がみられる(丸で囲まれた部分)．黄斑部局所ERG(c)では5度，10度，15度の刺激に対する応答がいずれも減弱している．

通常の視力検査と，手持ちの'字ひとつ視力'による検査で大きく差が出る場合がある．前項に症例提示した患者も同様のケースである．このような患者では，単に視力表の背景光を消したり検査室の照明を暗くしたりするだけで，視力が数段階上がる場合がある．

視野検査では中心比較暗点が検出される．ただしゴールドマン動的視野計では，進行例を除いて異常を検出できないことも多い．更にハンフリー自動視野計を用いた場合でも，'中心30-2'のプログラムでは中心比較暗点が明瞭に検出できず，'中心10-2'でようやく暗点が検

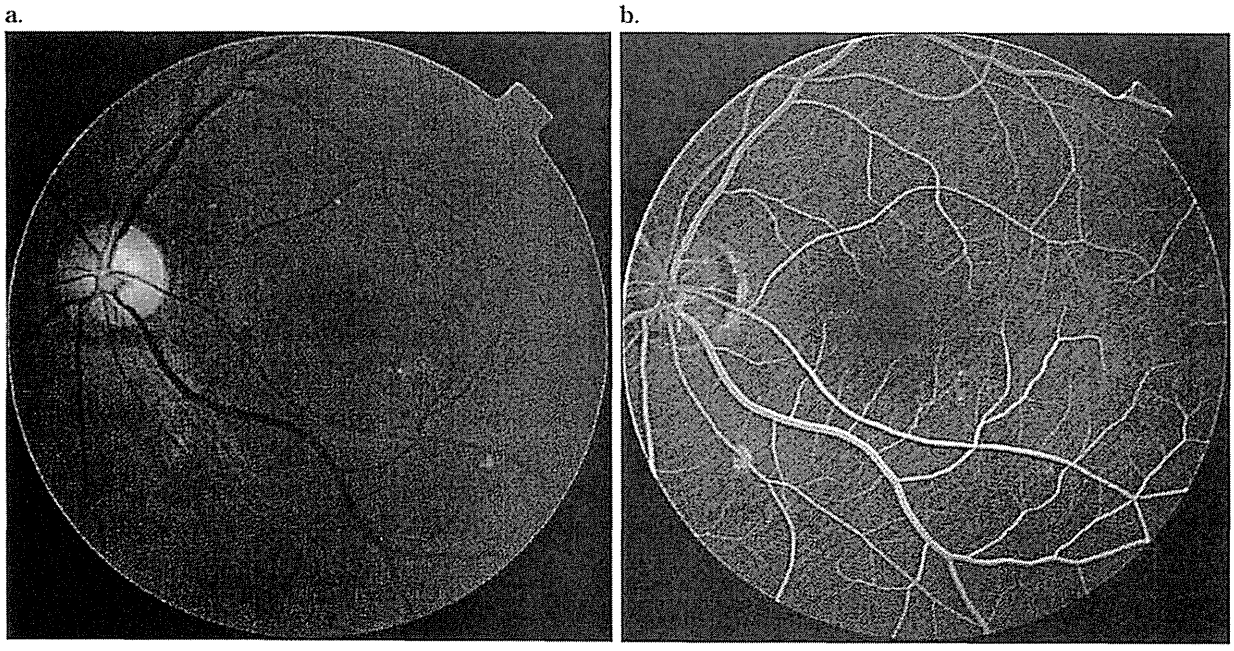

図4　三宅病患者(80歳，男性，*RP1L1* p.Arg45Trp heterozygous)の眼底(a)およびフルオレセイン眼底造影(b)
矯正視力は両眼とも0.2．発症後60年以上経過しているが，眼底黄斑部に異常所見はみられない．

出される例も多い．三宅病の進行をフォローするには，中心10度の視野と'中心窩閾値'を参考にするのが望ましい．なお，黄斑部以外の周辺視野は進行例でも正常に保たれている．

2) 他覚的検査

検眼鏡的所見，フルオレセイン蛍光眼底造影，インドシアニングリーン蛍光眼底造影ともにすべて正常である．若年者では，中心窩反射も明瞭に認められる(図2-a)．高齢に至っても網膜色素上皮の変性が現れることはない．経過中に黄斑部の変性が出現した場合には，三宅病の診断から除外される．

全視野ERGでは，杆体系，錐体系反応ともに正常に記録されるが，黄斑部局所ERGあるいは多局所ERGで黄斑部の反応が減弱しており，これが三宅病の確定診断となる(図3)．中心窩のごく狭い領域の機能が残存している場合は視力が正常なこともあるが，その場合でも黄斑部局所ERGや多局所ERGでは明らかな異常が検出される．

検眼鏡的所見は正常であるが，スペクトラルドメイン光干渉断層計(optical coherence tomography: OCT)で後極部を観察すると，比較的早い時期から網膜外層構造に異常をきたしていることがわかる[28]．初期の変化は，黄斑部における錐体視細胞外節先端部(cone outer segment tip: COST)ラインの消失，視細胞内節外節接合部(photoreceptor inner segment/outer segment junction: IS/OS)ラインの不明瞭化などである(図2-c)．OCTの所見は発症から長期間経過するにつれて次第に変化していく．すなわち，初期には中心窩のCOSTラインの消失およびIS/OSラインの境界不明瞭化(厚く，膨潤したように見える)がみられるが，中心窩網膜厚はほぼ正常である．更に長期間経過すると，中心窩でIS/OSラインの分断がみられるようになり，外顆粒層は菲薄化していく．正常視野領域に相当する黄斑部以外の視細胞構造は長期間経過しても正常であることが多いが，一部の症例ではIS/OSラインの不明瞭化がみられることもある．これらの形態変化は，*RP1L1*変異をもつ三宅病に共通にみられる所見である．

網膜自発蛍光は正常の場合が多いが(図2-b)，時に非特異的なごく弱い過蛍光が中心窩付近にみられることもある[25]．ただし，パターンジストロフィー，錐体・杆体ジストロフィー，

スターガルト病に特徴的な強い過蛍光や低蛍光の所見，リング状の異常所見などはみられないため，鑑別は容易である．

4. 三宅病と鑑別すべき疾患

眼底所見および全視野ERGが正常であるため，多くの患者が原因不明の視神経疾患，あるいは心因性視力障害などと診断されている．また比較的多いのが，白内障として眼内レンズ挿入術を施行されたあとに視力が改善せず，精査を依頼されて見つかるケースである．いずれの場合も，黄斑部のERGが局所的に低下していることさえ証明できれば診断は容易である．頭部CTやMRIを用いる必要もない．

なかなか正確な診断にたどり着かない一つの原因は，ひとたび視神経疾患や心因性視力障害を疑われてしまうと，その後に網膜専門医を受診する機会を失ってしまうことにあるようだ．網膜専門医以外にとって，多局所ERGや黄斑部局所ERGを施行するのはやや敷居が高いのかもしれない．ただし前述のように，スペクトラルドメインOCTを用いると黄斑部の異常を簡単にスクリーニングできるので，今後はより早く三宅病の診断に近づけるケースが増えていくことが期待される．

後述するが，孤発例の中には経過観察中に網膜色素上皮変性をきたす症例がまれにみられ，これは三宅病とは異なる黄斑症と考えられる．このような症例の場合，網膜自発蛍光を用いると網膜色素上皮の異常を早期にとらえることができる．

5. 三宅病の原因遺伝子

2010年に東京医療センターの研究チームを中心とした研究グループにより，優性遺伝タイプのオカルト黄斑ジストロフィーの原因遺伝子として8番短腕に位置する*RP1L1*が同定された(**図5**)[6]．これは国内の大家系における連鎖解析によって明らかにされたものである．これまでに45番目のアルギニンをトリプトファン(p.Arg45Trp)，および960番目のトリプトファンをアルギニン(p.Trp960Arg)に置き換える2つのミスセンス変異が見つかっている．なお，家系内には自覚症状がなく両眼の矯正視力が1.2という発症者も含まれており，連鎖解析にあたっては罹患者，非罹患者の鑑別が大変重要となった．このため調査にあたっては，症状のない家族も含めて全例で局所ERGおよびスペクトラルドメインOCTを施行し，かつ30歳以下の家族は正常サンプルに含めないなどの工夫を行った．

ヒトにおける*RP1L1*の機能はまだよく明らかにされていない．これまでの研究では，霊長類では錐体および杆体視細胞の特に内節に発現しており，視細胞内節・外節の構造維持，細胞内輸送に大きな役割を果たしていると考えられている[29,30]．

6. 孤発例の三宅病について

三宅らが1989年に最初に報告した症例は常染色体優性遺伝の家系であったが，その後は孤発例の報告も時折みられるようになってきている．もともとオカルト黄斑ジストロフィーという病名は，‘眼底所見が正常で，全視野ERGが正常かつ黄斑部局所ERGが異常であるジストロフィー’という病態を指していた．このため，一見同じ臨床検査所見を呈していても異なる原因の疾患が幾つか含まれている可能性がある．これまでの研究により，優性遺伝型の三宅病が*RP1L1*変異(p.Arg45Trp，p.Trp960Argあるいはp.Ser1199Cys)による視細胞異常を原因とすることが明らかになった．*RP1L1*遺伝子の異常を原因とする患者のOCT所見は，前述のように非常に特徴的な中心窩の視細胞異常を示している．一方*RP1L1*遺伝子に異常をもたない症例の多くについてOCT所見を観察すると，視細胞外節の萎縮が短期間で進行していたり，視細胞内節が比較的正常に保たれているなど，*RP1L1*変異の症例とは明らかに病態が異なると思われるケースが含まれている[28]．これらの疾患は，自覚的症状や電気生理学的な病態は同一でも，その疾患原因は全く別のところにあると考えられる．

現在のところ，三宅病とは‘両眼にゆっくり

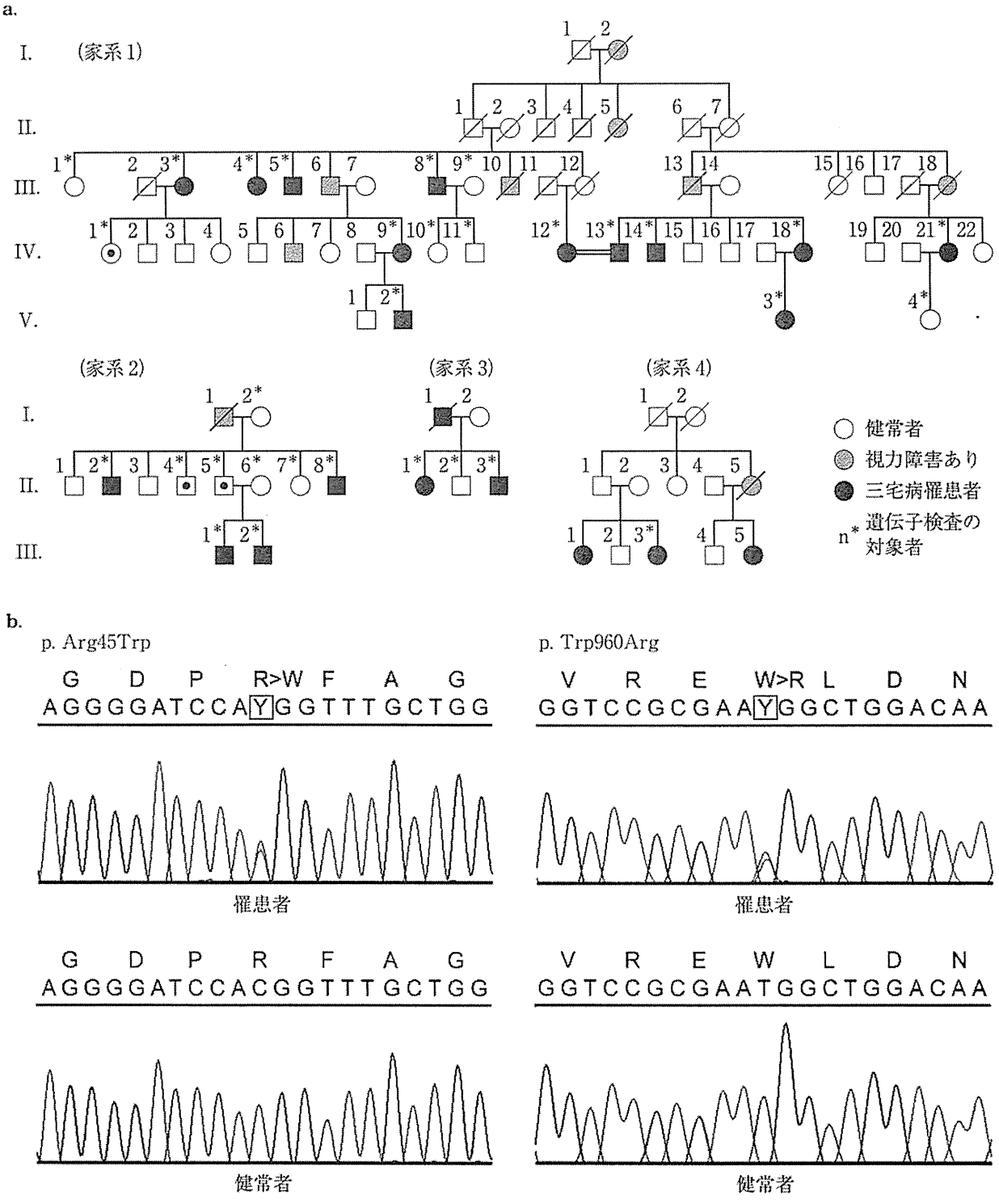

図5 三宅病の家系と*RP1L1*変異(文献[9]より改変)

a. 遺伝子異常のみられた三宅病家系．罹患者のすべてに*RP1L1*の変異が認められた．b. 上記家系でみられた2種類のミスセンス変異．

と進行する黄斑部に限局した視細胞障害で，血管や網膜色素上皮に異常のみられないもの'と定義される．この疾患の病態には*RP1L1*以外にも複数の原因(例えば劣性遺伝によるもの)が関与していると考えられ，今後の研究成果が待たれるところである．

7. 三宅病研究に残された謎

優性遺伝型の三宅病に*RP1L1*の変異が関与していることが明らかになったが，同時に新たな疑問点も生じている．*RP1L1*は霊長類の錐体視細胞だけでなく杆体視細胞にも発現しているが，三宅病で視細胞機能が低下するのは黄斑部に限られている．スペクトラルドメインOCTで三宅病の視細胞層を観察すると，発症から30年以上経過しても黄斑部以外の視細胞構造が正常に保たれている例が多い．なぜ，長期間経過しても杆体の機能が低下しないのか，黄斑部以外の錐体が障害を受けないのか．また，視細胞が変性，萎縮に陥っているにもかかわらず，なぜ網膜色素上皮は最後まで正常に保たれるのか．これらは錐体・杆体ジストロフィーなど，他の網膜疾患では一般にみられない所見である．

これらの疑問を解決するためには，ヒトにおける*RP1L1*発現の正確な局在を明らかにするだけでなく，遺伝子変異から視細胞の構造異常および機能異常に至るまでの詳細なメカニズムを今後の研究によって解明する必要がある．

おわりに

三宅病の発見に至る経緯から疾患の特徴，診断法，あるいは今後の研究課題についてまとめた．

謝辞　今回の総説執筆にあたり，平素より御指導頂いている愛知医科大学理事長，三宅養三先生に深謝致します．

■文　献

1) 小口忠太：一種の夜盲症について．日眼会誌 **11**: 123-130, 1907.
2) Dryja TP, et al: A point mutation of the rhodopsin gene in one form of retinitis pigmentosa. Nature **343**(6256): 364-366, 1990.
3) Fuchs S, et al: A homozygous 1-base pair deletion in the arrestin gene is a frequent cause of Oguchi disease in Japanese. Nat Genet **10**(3): 360-362, 1995.
4) Miyake Y, et al: Hereditary macular dystrophy without visible fundus abnormality. Am J Ophthalmol **108**: 292-299, 1989.
5) Miyake Y, et al: Occult macular dystrophy. Am J Ophthalmol **122**: 644-653, 1996.
6) Akahori M, et al: Dominant mutations in *RP1L1* are responsible for occult macular dystrophy. Am J Hum Genet **87**: 424-429, 2010.
7) Miyake Y: Electrodiagnosis of Retinal Diseases, Springer-Verlag, Tokyo, 2006.
8) 藤波　芳，角田和繁：黄斑ジストロフィの遺伝子異常．眼科 **53**: 239-255, 2011.
9) Hirose T, et al: Simultaneous recording of electroretinogram and visual evoked response. Focal stimulation under direct observation. Arch Ophthalmol **95**(7): 1205-1208, 1977.
10) Arden GB, Bankes JL: Foveal electroretinogram as a clinical test. Br J Ophthalmol **50**(12): 740, 1966.
11) 三宅養三：黄斑部局所ERGでなにが分かる？ 臨眼 **56**: 680-688, 2002.
12) Miyake Y, Awaya S: Stimulus deprivation amblyopia. Simultaneous recording of local macular electroretinogram and visual evoked response. Arch Ophthalmol **102**(7): 998-1003, 1984.
13) Miyake Y, et al: Local macular electroretinographic responses in idiopathic central serous chorioretinopathy. Am J Ophthalmol **106**(5): 546-550, 1988.
14) Miyake Y, et al: Oscillatory potentials in electroretinograms of the human macular region. Invest Ophthalmol Vis Sci **29**(11): 1631-1635, 1988.
15) Miyake Y, et al: Asymmetry of focal ERG in human macular region. Invest Ophthalmol Vis Sci **30**(8): 1743-1749, 1989.
16) Miyake Y, et al: Focal macular electroretinogram in X-linked congenital retinoschisis. Invest Ophthalmol Vis Sci **34**(3): 512-515, 1993.
17) Sutter EE, Tran D: The field topography of ERG components in man—I. The photopic luminance

response. Vision Res **32**: 433-446, 1992.
18) Piao CH, et al: Multifocal electroretinogram in occult macular dystrophy. Invest Ophthalmol Vis Sci **41**: 513-517, 2000.
19) Nakamura M, et al: A case of occult macular dystrophy accompanying normal-tension glaucoma. Am J Ophthalmol **135**: 715-717, 2003.
20) Kondo M, et al: Foveal thickness in occult macular dystrophy. Am J Ophthalmol **135**: 725-728, 2003.
21) Wildberger H, et al: Multifocal electroretinogram (mfERG) in a family with occult macular dystrophy (OMD). Klin Monatsbl Augenheilkd **220**: 111-115, 2003.
22) Lyons JS: Non-familial occult macular dystrophy. Doc Ophthalmol **111**: 49-56, 2005.
23) Brockhurst RJ, Sandberg MA: Optical coherence tomography findings in occult macular dystrophy. Am J Ophthalmol **143**: 516-518, 2007.
24) Lubinski W, et al: A 43-year-old man with reduced visual acuity and normal fundus: occult macular dystrophy—case report. Doc Ophthalmol **116**: 111-118, 2008.
25) Fujinami K, et al: Fundus autofluorescence in autosomal dominant occult macular dystrophy. Arch Ophthalmol **129**: 597-602, 2011.
26) Park SJ, et al: Morphologic photoreceptor abnormality in occult macular dystrophy on spectral-domain optical coherence tomography. Invest Ophthalmol Vis Sci **51**: 3673-3679, 2010.
27) Hanazono G, et al: Pattern-reversal visual-evoked potential in patients with occult macular dystrophy. Clin Ophthalmol **4**: 1515-1520, 2010.
28) Tsunoda K, et al: Clinical characteristics of occult macular dystrophy in family with mutation of RP1l1 gene. Retina **32**(6): 1135-1147, 2012.
29) Conte I, et al: Identification and characterisation of the retinitis pigmentosa 1-like 1 gene (*RP1L1*): a novel candidate for retinal degenerations. Eur J Hum Genet **11**: 155-162, 2003.
30) Yamashita T, et al: Essential and synergistic roles of RP1 and *RP1L1* in rod photoreceptor axoneme and retinitis pigmentosa. J Neurosci **29**: 9748-9760, 2009.

Outer Retinal Morphology and Visual Function in Patients With Idiopathic Epiretinal Membrane

Ken Watanabe, MD; Kazushige Tsunoda, MD, PhD; Yoshinobu Mizuno, MD; Kunihiko Akiyama, MD; Toru Noda, MD

Objective: To determine the relationship between the morphology of the fovea and visual acuity in patients with an untreated idiopathic epiretinal membrane (ERM).

Methods: We examined 52 eyes of 45 patients diagnosed with an ERM. The morphology of the foveal area was determined by spectral-domain optical coherence tomography. The relationships between the best-corrected visual acuity (BCVA) and 8 optical coherence tomography features, central retinal thickness, cone outer segment tip (COST) line, photoreceptor inner/outer segment (IS/OS) junction line, foveal bulge of the IS/OS line, external limiting membrane, inner limiting membrane, foveal pit, and ERM over the foveal center, were evaluated.

Results: Multiple regression analysis showed that intact COST line, IS/OS junction line, and external limiting membrane independently and significantly contributed to the BCVA. The standardized partial regression coefficient β was 0.415 for the COST line, 0.287 for the IS/OS junction line, and 0.247 for the external limiting membrane. However, the other features, eg, foveal bulge, inner limiting membrane, foveal pit, and ERM, were not significantly associated with the BCVA. The central retinal thickness was significantly correlated with the BCVA (r^2=0.274; $P<.01$).

Conclusions: At an early stage of an ERM, only the photoreceptor structures are significantly associated with the BCVA, and the appearance of the COST line was most highly associated. Detailed examinations of the photoreceptor structures using optical coherence tomography may help find photoreceptor dysfunction in cases of idiopathic ERM.

JAMA Ophthalmol. 2013;131(2):172-177

Author Affiliations: Department of Ophthalmology, National Tokyo Medical Center (Drs Watanabe, Akiyama, and Noda), and Laboratory of Visual Physiology, National Institute of Sensory Organs (Drs Tsunoda and Mizuno), Tokyo, Japan.

Optical coherence tomography (OCT) is a useful method of detecting early morphological changes in retinas affected by various pathological conditions. The correlations between the visual acuity and the morphological changes in the retina have been reported for various retinal diseases, such as age-related macular degeneration,[1] central serous chorioretinopathy,[2] macular edema,[3,4] idiopathic macular hole,[5,6] and epiretinal membrane (ERM).[7-9]

Retinal traction caused by an ERM leads to morphological changes of not only the superficial layers of the retina but also the entire retina including the photoreceptor layer. This is important because long-standing morphological changes can lead to functional damages and cause metamorphopsia and decreased visual acuity.

Spectral-domain OCT (SD-OCT) has enabled clinicians and investigators to obtain clearer images of the microstructure of the photoreceptor layer than time-domain OCT. Several studies have examined whether significant correlations exist between macular dysfunction and the integrity of photoreceptor microstructures, especially the photoreceptor inner segment/outer segment (IS/OS) junction line, detected by SD-OCT in patients with an ERM.[7-10]

The diagnostic value of determining the integrity of the IS/OS junction line and the cone outer segment tip (COST) line by SD-OCT has been done primarily on diseases of the outer retina, eg, acute zonal occult outer retinopathy[11] and hereditary macular dystrophies.[12-14] However, in eyes with an ERM, the appearance of the photoreceptor microstructures in the SD-OCT image can be affected by retinal thickening, subretinal cysts, and the ERM itself. These alterations lead to a reduction in the intensity of the laser light reaching the photoreceptor layer. In addition, the clarity of the SD-OCT images of the outer retina, eg, the Henle layer, IS/OS junction line, and COST line, is dependent on the incidence angle of the laser beam on the retina, which would be altered by an ERM.[15,16] Thus, the diagnostic value of examining the photoreceptor microstructures by SD-OCT in eyes with an ERM may not be as reliable as in cases of acute zonal occult outer retinopathy and other outer retinal diseases where the inner retinal alterations do not attenuate the laser energy.

The purpose of this study was to evaluate the relationship between deteriora-

tion of the best-corrected visual acuity (BCVA) and abnormalities of the photoreceptor microstructures in patients with untreated idiopathic ERM. To accomplish this, we examined cases with ERM without severely deformed inner structures, such as a lamellar hole and large cystic formations. We classified the abnormalities of the retina in the SD-OCT images and performed multiple regression analyses to determine which parameter was independently and significantly associated with the BCVA in cases of ERM.

METHODS

This was a retrospective case series performed in the Department of Ophthalmology, National Tokyo Medical Center, Tokyo, Japan. After an explanation of the procedures to be used, an informed consent was received from all of the subjects for the tests. The procedures used adhered to the tenets of the Declaration of Helsinki, and approval to perform this study was obtained from the review board/ethics committee of the Tokyo Medical Center.

We examined 52 eyes of 45 patients (20 eyes of 18 men and 32 eyes of 27 women, mean [SD] age, 67.0 [10.0] years) diagnosed with an ERM without lamellar holes or apparent cystic changes in the fovea. The patients were examined between October 2009 and September 2010. The exclusion criteria were myopia more than 6 diopters, advanced lens opacification, other ocular disease that could cause visual disturbances, secondary ERM caused by vascular diseases, uveitis, and retinal detachment. Cases whose OCT images did not have enough signal intensity for evaluation, ie, average intensity of the SD-OCT signal was less than 8 of 10, were also excluded.

Spectral-domain OCT (Cirrus HD-OCT, versions 4.5 and 5.1; Carl Zeiss Meditec) was used to obtain tomographic images of the retina. Following dilation of the pupil, 5 line-scan images were obtained both horizontally (length, 9.0 mm) and vertically (length, 6.0 mm) across the foveola, with the distance between each scan line of 0.075 mm. Cases where any of the scan lines did not pass through the foveola were excluded.

Eight SD-OCT features were evaluated: (1) central retinal thickness (CRT), (2) COST line, (3) IS/OS junction line, (4) bulgelike appearance of the IS/OS junction line at the foveola (foveal bulge), (5) external limiting membrane (ELM), (6) internal limiting membrane (ILM), (7) foveal pit, and (8) ERM formation over the foveal center.

The CRT was defined as the distance between the inner retinal surface and inner surface of the retinal pigment epithelium at the foveola (**Figure 1**A). It was measured manually by the built-in scale of the SD-OCT system.

The microstructures within a 500-μm diameter of the fovea (Figure 1A, scale bar) were graded independently by 2 experienced ophthalmologists (K.W. and K.T.) (**Table 1**) to be either normal or abnormal. During this procedure, all the patients' information, including the BCVA, was masked to the examiners. In cases where the gradings were different, discussions were held until both examiners agreed. In earlier studies, the OCT features were graded into 3 classes, eg, normal ILM, mild ILM distortion, and severe ILM distortion.[9,11] We initially adopted a similar classification; however, we found it confusing especially in distinguishing mildly from severely abnormal structures. We have thus simplified the classification to normal or abnormal.

The COST line, IS/OS junction line, and ELM were graded normal when they were seen clearly and appeared continuous in the foveal region, and they were graded abnormal when they were blurred, interrupted, or absent. The foveal bulge is an elevation of the IS/OS junction line that appears like a dome over the foveola. We graded it normal when the bulgelike appearance was clearly observed and graded it abnormal when the bulgelike appearance was not observed and the IS/OS junction line appeared flat.

The ILM was graded normal when it looked smooth and flat at the fovea and was graded abnormal when it looked wrinkled or distorted. The foveal pit was graded normal when the concave retinal surface was clearly observed at the foveola and graded abnormal when the foveal surface appeared flat. The ERM was graded normal when the ERM did not overlap the foveola and graded abnormal when the ERM was attached over the foveola.

The relationship between these 8 OCT features and the visual acuity was statistically examined. Statistical analysis was performed using SPSS version 19.0 (SPSS Japan). The visual acuity was converted to logMAR units for the statistical analyses. Pearson correlations were performed to determine the association between CRT and visual acuity. The Mann-Whitney test was used to compare the BCVA and CRT between the normal and abnormal groups for each OCT feature. Multiple regression analysis was performed with BCVA and CRT as the dependent variables and with the integrities of 7 OCT features as independent variables. A P value $< .05$ was considered significant.

RESULTS

We first evaluated the normal fellow eyes of 29 of the 45 patients studied (13 eyes of 13 men and 16 eyes of 16 women; mean [SD] age, 66.0 [8.1] years). For these, all of the 7 OCT features were judged normal.[15]

Two representative cases demonstrating how the OCT features were judged to be either normal or abnormal are shown in Figure 1B and C. A horizontal SD-OCT scan image of the left retina of a 74-year-old man is shown in Figure 1B. The ELM, foveal bulge, IS/OS junction line, and COST line were clearly observed and judged to be normal. An ERM was present over the foveola, and this was judged to be abnormal. The foveal pit was concave and judged to be normal. The ILM was partially wrinkled at the foveola and judged abnormal.

A vertical SD-OCT scan image of the right retina of a 63-year-old woman is shown in Figure 1C. The IS/OS junction line and ELM were clearly observed and judged to be normal. The foveal bulge and COST line could not be seen at the fovea and were judged abnormal. The ILM was wrinkled in the parafoveal region; however, the foveal region within 500 μm of the foveola was spared and judged normal. The foveal pit was judged abnormal because the fovea was elevated by a tangential traction from the ERM and the foveal pit was flattened. An ERM covered the foveola and was judged abnormal.

The BCVA and CRT of the normal eyes were compared with those of the abnormal groups for each OCT feature of the 52 cases by Mann-Whitney test (**Figure 2**). The BCVA was significantly better in cases when 6 OCT features were judged to be normal: COST line, IS/OS junction line, foveal bulge, ELM, foveal pit, and ERM (Figure 2A). The CRT was significantly thinner in cases when 5 OCT features were judged to be normal: COST line, IS/OS junction line, foveal bulge, foveal pit, and ERM (Figure 2B).

Subsequently, multiple regression analyses were performed to determine the independent predictors of the BCVA and CRT in eyes with an ERM. The analyses showed

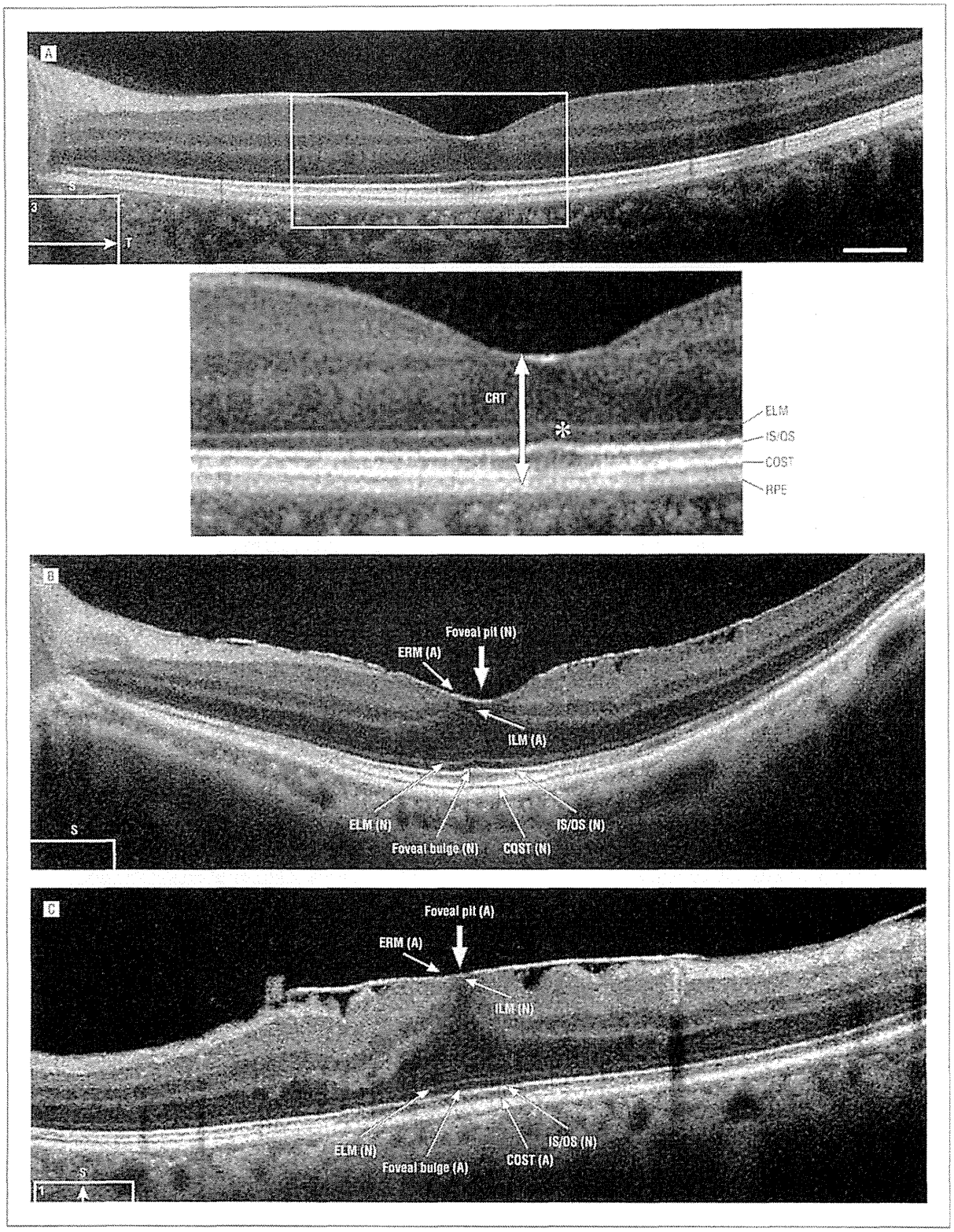

Figure 1. Optical coherence tomography images. A, Horizontal optical coherence tomography image of the retina of a normal eye with a magnified image showing the locations of the external limiting membrane (ELM), photoreceptor inner segment/outer segment junction line (IS/OS), cone outer segment tip line (COST), retinal pigment epithelium (RPE), foveal bulge (asterisk), and central retinal thickness (CRT) (arrow). Scale bar = 500 μm. B and C, Classification of 7 features in spectral-domain optical coherence tomography image in patients with an epiretinal membrane (ERM). A indicates abnormal; ILM, internal limiting membrane; and N, normal.

Table 1. Classification of OCT Features in the Foveal Region

Classification	COST	IS/OS	Foveal Bulge	ELM	ILM	Foveal Pit	ERM
Normal	Clear and continuous	Clear and continuous	Observed	Clear and continuous	Smooth and flat	Observed	Foveola is free of ERM
Abnormal	Blurred, interrupted, or absent	Blurred, interrupted, or absent	Not observed	Blurred, interrupted, or absent	Wrinkled or distorted	Not observed	ERM is attached over foveola

Abbreviations: COST, cone outer segment tip line; ELM, external limiting membrane; ERM, epiretinal membrane; ILM, internal limiting membrane; IS/OS, photoreceptor inner segment/outer segment junction line; OCT, optical coherence tomography

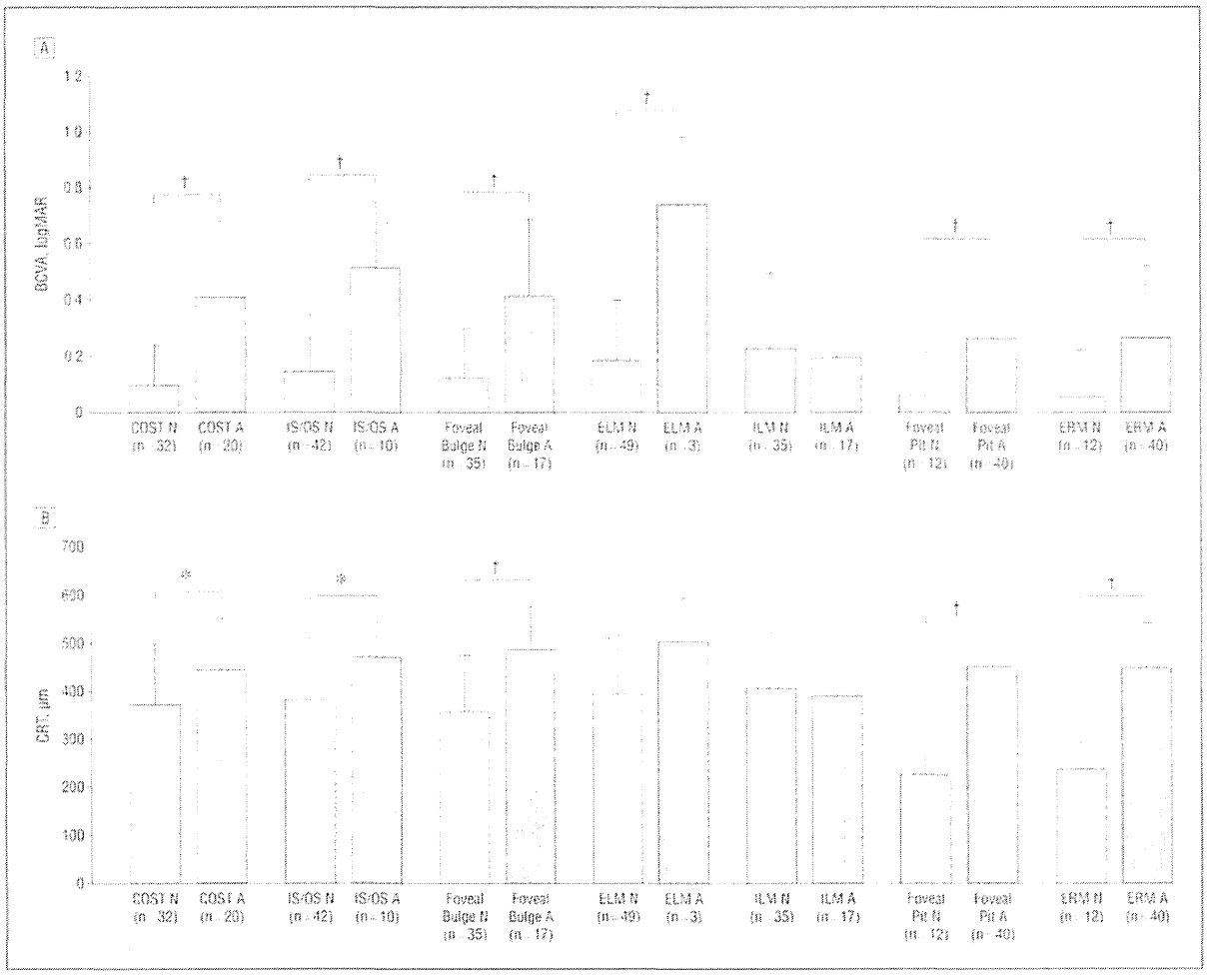

Figure 2. Comparisons between normal (N) and abnormal (A) eyes for 7 optical coherence tomography features. A, Best-corrected visual acuity (BCVA). B, Central retinal thickness (CRT). Mann-Whitney test, *$P < .05$ and †$P < .01$. COST indicates cone outer segment tip line; ELM, external limiting membrane; ERM, epiretinal membrane; ILM, internal limiting membrane; and IS/OS, inner segment/outer segment junction line.

that the predictive variables for BCVA were COST line ($P < .001$), IS/OS junction line ($P = .02$), and ELM ($P = .03$). The standardized partial regression coefficient β was 0.415 for the COST line, 0.287 for the IS/OS junction line, and 0.247 for the ELM (**Table 2**). On the other hand, the predictive variables for the CRT were foveal pit ($P < .001$), ERM ($P = .003$), and foveal bulge ($P = .04$). The standardized partial regression coefficient β was 0.476 for the foveal pit, 0.337 for the ERM, and 0.182 for the foveal bulge (**Table 3**).

The CRT was measured at the foveal center in 52 cases, and a significantly positive correlation was observed between the CRT and the BCVA ($r^2 = 0.274$; $P < .01$) (**Figure 3**).

COMMENT

The relationships between the outer retinal microstructures determined by SD-OCT and the BCVA have been reported previously for patients with ERM.[7-10] The de-

Table 2. Multiple Regression Analyses to Determine the Independent Predictors of the Best-Corrected Visual Acuity

	Standardized Partial Regression Coefficient (β)	*P* Value
COST	0.415	<.001
IS/OS	0.287	.02
ELM	0.247	.03

Abbreviations: COST, cone outer segment tip line; ELM, external limiting membrane; IS/OS, photoreceptor inner segment/outer segment junction line.

Table 3. Multiple Regression Analyses to Determine the Independent Predictors of the Central Retinal Thickness

	Standardized Partial Regression Coefficient (β)	*P* Value
Foveal pit	0.476	<.001
ERM	0.337	.003
Foveal bulge	0.182	.04

Abbreviation: ERM, epiretinal membrane.

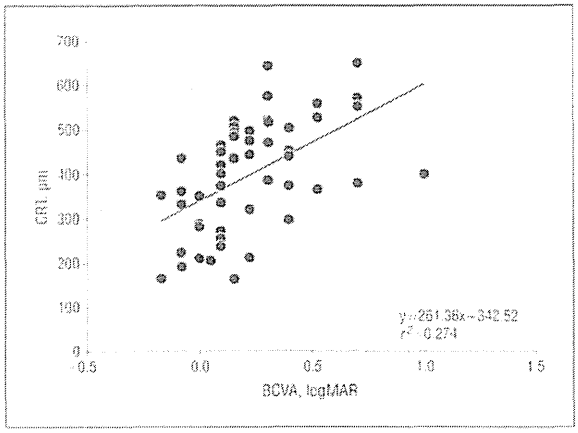

Figure 3. Significant correlation between central retinal thickness (CRT) and best-corrected visual acuity (BCVA) in 52 eyes. Pearson correlation coefficient r^2 was 0.274 ($P < .01$).

sign of our study was different from these earlier studies because we evaluated the OCT features only in the foveal region within 500 μm of the center because the visual acuity is mainly determined by the foveal center. In addition, we excluded patients who had small lamellar holes or apparent cystic changes in the fovea, which can induce optical artifacts and distort the appearances of the photoreceptor layer in the OCT images.

Multiple regression analyses showed that the integrity of the COST line was most strongly associated with the BCVA, followed by the IS/OS junction line and the ELM. On the other hand, the foveal bulge, ILM, foveal pit, and ERM were not significantly associated with the BCVA. It has been reported that the integrity of the IS/OS junction line is significantly associated with the postoperative BCVA.[7,8] Our results showed that not only the IS/OS junction but also the COST line were most strongly associated with the preoperative BCVA (β = 0.415 for COST line; β = 0.287 for IS/OS junction). Abnormalities of the COST line have been suggested to be an early sign of photoreceptor dysfunction in eyes with outer retinal disorders.[13-16] In cases of ERM, the appearance of the COST line at the fovea should be carefully examined to determine if early changes in retinal function might be present.

In patients with an ERM, the retinal thickening could affect the appearance of the images of the photoreceptor layer. Multiple regression analysis showed that abnormalities in the COST line, IS/OS junction line, and ELM were not significantly associated with the CRT (Table 2 and Table 3), although an absence of the foveal pit ($P < .001$) and existence of foveal ERM over the foveola ($P = .003$) were independently associated with the CRT. These results suggest that the photoreceptor microstructures appeared abnormal not because of the reduced laser light through thickened retina but because of real morphological changes. The abnormality in the inner retinal structures, eg, ILM, foveal pit, and ERM at the foveola, might affect the visual acuity because they would alter the optical characteristics of the retina. However, the results of multiple regression analysis showed that these inner retinal abnormalities did not significantly contribute to the BCVA at least in the early stage of ERM.

The correlations between the 4 highly refractive bands in the outer retina seen in the SD-OCT images and the retinal histologic features have been well investigated.[16,20-23] There has been an early consensus on the interpretation of the first and fourth bands in the outer retina, the innermost band representing the ELM and the outermost band representing the complex of the retinal pigment epithelium and Bruch membrane. The second band was initially thought to arise from the differences in the refractive index between the inner and outer segments of the photoreceptor and thus called the photoreceptor IS/OS junction line. However, Fernández et al[21] found it to represent the ellipsoids of the photoreceptor inner segment by ultra high-resolution OCT with adaptive optics. The third band has been found to represent the junction between the cone outer segment and the apical microvillae of the retinal pigment epithelium and is called the COST line.[16,21] The ellipsoids in the photoreceptor inner segments are rich in mitochondria and crucial for the metabolism of the photoreceptors. The cone outer segments contain the photopigment discs, which are also important for phototransduction. The strong contributions of the COST and IS/OS junction lines to the BCVA but not to the CRT suggest that both the microstructure and function of the photoreceptors were damaged by the ERM.

The OCT abnormalities in the photoreceptor microstructures have been reported to be significantly correlated with the loss of visual acuity and visual field in acute zonal occult outer retinopathy and retinal dystrophies where the photoreceptors are primarily affected.[13-15] On the other hand, the abnormal ERM develops on the surface of the retina without directly affecting the photoreceptor layer. The membrane can then cause tangential traction over the macula, followed by an inward traction toward the vitreous cavity at the foveal pit. Long-standing inward traction may cause formations of cysts in the outer nuclear layer

and microstructural changes in the photoreceptor.[7,8,22,23] Thus, the etiology of the OCT abnormalities of the photoreceptor layer observed in eyes with an ERM should be different from that of outer retinal diseases.

Niwa et al[24] measured focal macular electroretinograms (fmERGs) elicited by 15° stimuli in 37 patients with an ERM and concluded that the inner retinal layer was predominantly impaired initially and that the visual dysfunction in eyes with ERM may have resulted from macular edema. They also found that the correlation between the visual acuity and the degree of amplitude reduction of the a wave, b wave, and oscillatory potentials was not significant. However, they reported that the visual acuity largely depended on a very limited region of the fovea, and the stimulated region of 15° in the fmERG was too large to evaluate the relationship between the BCVA and fmERGs. In fact, there are patients with macular dystrophy who have both good visual acuity and extinguished fmERGs.[19] In such patients, the function of a very small region of the fovea is spared. In cases of ERM, an inward traction is especially strong in the foveola as shown in Figure 1B and C, and the outer nuclear layer within 500 μm of the foveola is thicker than in the parafoveal region. Thus, the results of fmERGs elicited by 15° stimuli did not necessarily exclude the fact that the photoreceptor function was primarily affected by the ERM. Considering that mechanical traction is extraordinarily severe in the foveola, the photoreceptor function may be primarily impaired even at the early stage of ERM, leading to the reduction of the BCVA.

There are reports that the reduction in the visual acuity in eyes with an ERM is due to retinal thickening,[9,10] and our results also indicated that the thickness of the outer retina, ie, combined thickness of outer nuclear layer and photoreceptor layer, was correlated with visual acuity (Figure 3). Together with the results of multiple regression analysis, functional damage of the photoreceptor due to long-standing inward traction was determined to be a strong contributor to the visual acuity reduction. Thus, detailed examinations of the photoreceptor microstructures in the OCT images may help find early visual dysfunction in cases of idiopathic ERM.

Submitted for Publication: July 4, 2012; accepted July 19, 2012.

Correspondence: Kazushige Tsunoda, MD, PhD, Laboratory of Visual Physiology, National Institute of Sensory Organs, 2-5-1 Higashigaoka, Meguro-ku, Tokyo 152-8902, Japan (tsunodakazushige@kankakuki.go.jp).

Conflict of Interest Disclosures: None reported.

Funding/Support: This research is supported in part by research grants from the Ministry of Health, Labor, and Welfare, Japan, and Grant-in-Aid for Scientific Research, Japan Society for the Promotion of Science.

REFERENCES

1. Keane PA, Liakopoulos S, Chang KT, et al. Relationship between optical coherence tomography retinal parameters and visual acuity in neovascular age-related macular degeneration. *Ophthalmology.* 2008;115(12):2206-2214.
2. Piccolino FC, de la Longrais RR, Ravera G, et al. The foveal photoreceptor layer and visual acuity loss in central serous chorioretinopathy. *Am J Ophthalmol.* 2005; 139(1):87-99.
3. Otani T, Yamaguchi Y, Kishi S. Correlation between visual acuity and foveal microstructural changes in diabetic macular edema. *Retina.* 2010;30(5):774-780.
4. Ota M, Tsujikawa A, Murakami T, et al. Foveal photoreceptor layer in eyes with persistent cystoid macular edema associated with branch retinal vein occlusion. *Am J Ophthalmol.* 2008;145(2):273-280.
5. Itoh Y, Inoue M, Rii T, Hiraoka T, Hirakata A. Significant correlation between visual acuity and recovery of foveal cone microstructures after macular hole surgery. *Am J Ophthalmol.* 2012;153(1):111-119, e1.
6. Wakabayashi T, Fujiwara M, Sakaguchi H, Kusaka S, Oshima Y. Foveal microstructure and visual acuity in surgically closed macular holes: spectral-domain optical coherence tomographic analysis. *Ophthalmology.* 2010;117(9):1815-1824.
7. Falkner-Radler CI, Glittenberg C, Hagen S, Benesch T, Binder S. Spectral-domain optical coherence tomography for monitoring epiretinal membrane surgery. *Ophthalmology.* 2010;117(4):798-805.
8. Suh MH, Seo JM, Park KH, Yu HG. Associations between macular findings by optical coherence tomography and visual outcomes after epiretinal membrane removal. *Am J Ophthalmol.* 2009;147(3):473-480, e3.
9. Michalewski J, Michalewska Z, Cisiecki S, Nawrocki J. Morphologically functional correlations of macular pathology connected with epiretinal membrane formation in spectral optical coherence tomography (SOCT). *Graefes Arch Clin Exp Ophthalmol.* 2007;245(11):1623-1631.
10. Arichika S, Hangai M, Yoshimura N. Correlation between thickening of the inner and outer retina and visual acuity in patients with epiretinal membrane. *Retina.* 2010;30(3):503-508.
11. Tsunoda K, Fujinami K, Miyake Y. Selective abnormality of cone outer segment tip line in acute zonal occult outer retinopathy as observed by spectral-domain optical coherence tomography. *Arch Ophthalmol.* 2011;129(8):1099-1101.
12. Sergouniotis PI, Holder GE, Robson AG, Michaelides M, Webster AR, Moore AT. High-resolution optical coherence tomography imaging in KCNV2 retinopathy. *Br J Ophthalmol.* 2012;96(2):213-217.
13. Genead MA, Fishman GA, Rha J, et al. Photoreceptor structure and function in patients with congenital achromatopsia. *Invest Ophthalmol Vis Sci.* 2011;52 (10):7298-7308.
14. Hood DC, Zhang X, Ramachandran R, et al. The inner segment/outer segment border seen on optical coherence tomography is less intense in patients with diminished cone function. *Invest Ophthalmol Vis Sci.* 2011;52(13):9703-9709.
15. Lujan BJ, Roorda A, Knighton RW, Carroll J. Revealing Henle's fiber layer using spectral domain optical coherence tomography. *Invest Ophthalmol Vis Sci.* 2011; 52(3):1486-1492.
16. Srinivasan VJ, Monson BK, Wojtkowski M, et al. Characterization of outer retinal morphology with high-speed, ultrahigh-resolution optical coherence tomography. *Invest Ophthalmol Vis Sci.* 2008;49(4):1571-1579.
17. Mitamura Y, Hirano K, Baba T, Yamamoto S. Correlation of visual recovery with presence of photoreceptor inner/outer segment junction in optical coherence images after epiretinal membrane surgery. *Br J Ophthalmol.* 2009;93(2):171-175.
18. Rii T, Itoh Y, Inoue M, Hirakata A. Foveal cone outer segment tips line and disruption artifacts in spectral-domain optical coherence tomographic images of normal eyes. *Am J Ophthalmol.* 2012;153(3):524-529, e1.
19. Tsunoda K, Usui T, Hatase T, et al. Clinical characteristics of occult macular dystrophy in family with mutation of RP1l1 gene. *Retina.* 2012;32(6):1135-1147.
20. Spaide RF, Curcio CA. Anatomical correlates to the bands seen in the outer retina by optical coherence tomography: literature review and model. *Retina.* 2011; 31(8):1609-1619.
21. Fernández EJ, Hermann B, Povazay B, et al. Ultrahigh resolution optical coherence tomography and pancorrection for cellular imaging of the living human retina. *Opt Express.* 2008;16(15):11083-11094.
22. Wilkins JR, Puliafito CA, Hee MR, et al. Characterization of epiretinal membranes using optical coherence tomography. *Ophthalmology.* 1996;103(12): 2142-2151.
23. Gaudric A. Macular cysts, holes and cavitations: 2006 Jules Gonin lecture of the Retina Research Foundation. *Graefes Arch Clin Exp Ophthalmol.* 2008;246 (7):1071-1079.
24. Niwa T, Terasaki H, Kondo M, Piao CH, Suzuki T, Miyake Y. Function and morphology of macula before and after removal of idiopathic epiretinal membrane. *Invest Ophthalmol Vis Sci.* 2003;44(4):1652-1656.